Progress In Electromagnetics Research C, Vol. 44, 55–66, 2013

COMPLEX RECTANGULAR FILTER DESIGN USING HYBRID FINITE ELEMENT METHOD AND MODIFIED MULTIMODAL VARIATIONAL FORMULATION

Mohamed Yahia[1, *], Jun W. Tao[2], and Hédi Sakli[3]

[1]Systéme PV, Eoliens et Géothermaux, Ecole Nationale d'Ingénieurs de Gabés, Rue Omar Ibn Elkhattab, Gabès 6029, Tunisia

[2]Laboratoire Plasma et Conversion d'Energie LAPLACE, Ecole Nationale Supérieure d'Electrotechnique, d'Electronique, d'Informatique, d'Hydraulique et des Télécommunications, 2 rue Camichel, Toulouse cedex 31071, France

[3]Laboratoire SYSCOM, ENIT, BP.37, Tunis le Belvédère 1002, Tunisia

Abstract—We hybridize vector Finite Element Method (FEM) and a Modified Multimodal Variational Formulation (MMVF) to the accurate and fast design of complex isotropic rectangular filters. The MMVF is applied to the full-wave description in the rectangular waveguides while the FEM characterizes waves in the arbitrarily shaped discontinuities. The proposed hybrid method is applied to the full-wave analysis of circuits with great practical interest (i.e., cross-shaped iris and multimode filters), thus improving CPU time and memory storage against several full-wave FEM based Computer Aided Design (CAD) tools (i.e., HFSS High Frequency Structural Simulator). The performances of the proposed hybrid method are validated with experimental results and HFSS simulations.

1. INTRODUCTION

Several electromagnetic CAD tools for devices in millimeter waves and microwave have been developed in the last three decades. The modal methods such as the Mode Matching (MM) technique [1], the Generalized Scattering Matrix (GSM) analysis [2] and the Multimodal Variational Method (MVM) [3], use a modal development of electromagnetic fields on the basis of eigenmodes of constituent waveguides.

Received 29 July 2013, Accepted 16 September 2013, Scheduled 18 September 2013
* Corresponding author: Mohamed Yahia (mohamed_yahia1@yahoo.fr).

Generally, when we use modal methods as in [2, 3], the size of the scattering matrix depends on the total number of modes in the input and the output of the circuits. In our multimodal variational formulation [3], the size of the scattering matrix depends only on the number of accessible modes, which is independent from the total number of modes used; this contributes to an accurate description of the electromagnetic field near the discontinuities in form of series terms, without modifying the final scattering S matrix. Hence, reducing the size of the scattering matrix minimizes the memory storage and the computational time compared to other modal methods such us MM and GSM.

Classically, when analyzing cascaded discontinuities, the S matrix of each discontinuity is determined in advance. The response of the complete circuit is obtained by connecting all S matrices through the respective waveguides. Thus, the choice of the number of accessible modes in the study of intermediate discontinuities must be judicious. Consequently, a convergence study should be taken to insure the accuracy of the overall S matrix especially when the discontinuities are closer or the fundamental mode is degenerated. To avoid this convergence study, a Modified Multimodal Variational Formulation (MMVF) has been proposed [4] to study simple cascaded discontinuities. Instead of variational forms established at each discontinuity as in [3], a global variational form depending on a vector of electric fields including all discontinuities has been derived. Consequently, the size of the global scattering matrix depends only on the number of accessible modes in the beginning and the end of the overall structure.

However, when a waveguide of arbitrarily-shaped cross section is involved, the modal basis is no more analytical and the numerical determination of eigenvalues and eigenvectors will increase considerably the CPU time. The use of space meshing techniques, i.e., FEM [5], produces accurate results. Nevertheless, these techniques require important CPU time and memory storage. To alleviate these drawbacks, several hybrid methods that combine modal and space meshing methods such like hybrid FEM-MM have been proposed for waveguide problems [6–12].

In [13], we presented a hybrid FEM-MVM tool to the studying of complex discontinuities in rectangular vacuum waveguides. In [14], we generalized the hybrid method proposed in [13] to analyze cascaded uniaxial complex 2D discontinuities.

In this paper, we hybridize vector the FEM and the MMVF to the accurate and fast design of complex isotropic rectangular filters. We illustrate the advantages of the proposed hybrid method against several CAD tools with details. The analysis program is developed in Matlab on a PC (Intel Core 2 Duo, 2.66 GHz and 3-GB RAM).

2. THEORY

We consider multiple uniaxial complex 2D discontinuities between rectangular waveguides in isotropic medium as shown in Fig. 1 where S_i represents the aperture of the ith discontinuity. ε_r and μ_r denote the relative permittivity and the relative permeability of the medium, respectively. In the case of simple discontinuities between waveguides, the MMVF provides a full-wave characterization of the complete structure [4]. Its principle is to minimize the following variational and stationary function [4]:

$$f(E_t) = \left\langle \begin{pmatrix} E_{t1} & E_{t2} & \ldots & E_{tM} \end{pmatrix} \middle| \hat{Y} \begin{pmatrix} E_{t1} \\ E_{t2} \\ \vdots \\ E_{tM} \end{pmatrix} \right\rangle \tag{1}$$

$\langle . \mid . \rangle$ denotes the inner product, M the number of uniaxial discontinuities, and $\hat{Y}$ the self-adjoint admittance matrix operator of the complete structure [4]. When considering simple S_i apertures (i.e., rectangle, circle, ellipse, etc.) the tangential electrical field E_{ti} within the ith discontinuity can be expanded over the modal eigenfunction basis that satisfies the boundary conditions. When considering multiple complex S_i apertures as in Fig. 1, the determination of the modal eigenfunction basis is no longer obvious. To surmount this deficiency, we expressed the tangential electrical field E_{ti} as in the FEM edge formulation [13]. Each complex S_i aperture is divided into triangular elements. The tangential electric field within the linear

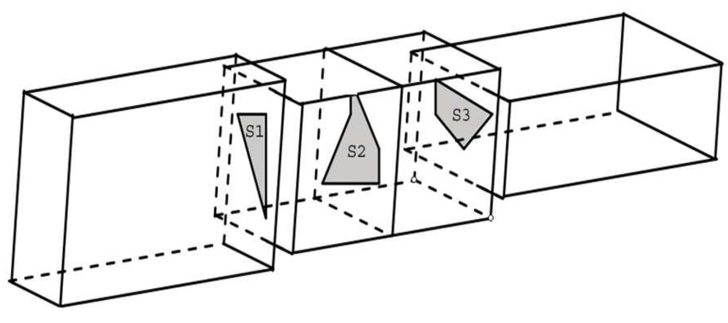

Figure 1. Waveguide filter with cascaded complex discontinuities.

triangular element (e) can be expressed as follows [5]:

$$E_t^e(x, y) = \sum_{m=1}^{3} E_m^e N_m^e(x, y) \quad x, y \in e \tag{2}$$

$N_m^e(x, y)$ are the interpolation functions and E_m^e the tangential electric fields along the mth edge. In this paper, we choose first order interpolation functions. After imposing the continuity condition between two adjacent elements, the tangential electric field within the S_i aperture can be expressed as follows [13]:

$$E_{ti}(x, y) = \sum_{pi=1}^{Ni} B_{pi} g_{pi}(x, y) \tag{3}$$

Ni denotes the number of edges in the S_i aperture and B_{pi} the unknown tangential electric field along the pth edge. To determine $g_{pi}(x, y)$, we have two cases:

- If the pth edge is in the boundary of the S_i aperture:

$$g_{pi}(x, y) = N_m^e(x, y) \quad x, y \in e \tag{4}$$

- If the pth edge is inside the S_i aperture, it can belongs only to two adjacent elements (e) and (e'). Consequently, the edge will define two interpolation functions $N_m^e(x, y)$ and $N_{m'}^{e'}(x, y)$ which have opposite directions [5]. Thus:

$$g_{pi}(x, y) = N_m^e(x, y) - N_{m'}^{e'}(x, y) \quad x, y \in \{e, e'\} \tag{5}$$

By combining (1) and (3), we obtain the following function:

$$f(E_t) = \left\langle \left(\sum_{p_1=1}^{N_1} B_{p_1} g_{p_1}(x, y) \ \ldots \ \sum_{p_M=1}^{N_M} B_{p_M} g_{p_M}(x, y) \right) \right| \hat{Y} \left(\begin{array}{c} \sum_{q_1=1}^{N_1} B_{q_1} g_{q_1}(x, y) \\ \vdots \\ \sum_{q_M=1}^{N_M} B_{q_M} g_{q_M}(x, y) \end{array} \right) \right\rangle \tag{6}$$

The scattering matrix of the complete circuit is obtained by minimizing the expression (6) with respect to B_{pi}. The size of the basis functions depends only on the number of edges Ni in the ith discontinuity which is different of the number of modes used. So that, we only manipulate matrices of sizes $Ni \times Ni$.

3. RESULTS

3.1. One Uniaxial Discontinuity $M = 1$: A Cross-shaped Iris

We consider a centred cross-shaped iris with rounded corners in a rectangular X-band WR90 waveguide. Fig. 2 shows the geometries and the meshing of the aperture. Fig. 3 displays the relative susceptances of the cross-shaped iris inserted in two isotropic media ($\varepsilon_r = 1$, $\mu_r = 1$) and ($\varepsilon_r = 1.5$, $\mu_r = 1.5$), respectively. Where B and Y_0 denote the susceptance of the cross-shaped aperture and the characteristic admittance respectively [15].

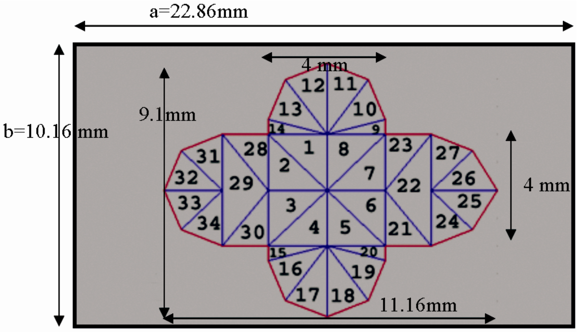

Figure 2. Geometries and meshing of the cross-shaped aperture.

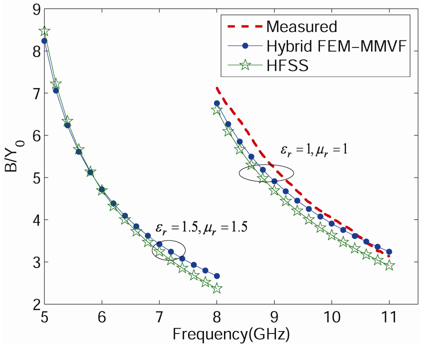

Figure 3. Relative susceptance of the cross-shaped iris.

We observe that the results of our method agree well with those obtained by measure and Ansoft HFSS commercial software. Nevertheless, the proposed hybrid method gives an overall reduction in CPU time more than 95% against HFSS in both cases. Convergence studies of results of our method against the number of elements and the number of modes in unfilled waveguide can be found in [13]. Table 1 gives a comparison in time between our hybrid method and HFSS using ($\varepsilon_r = 1$, $\mu_r = 1$) [13]. We mention that for one discontinuity the hybrid FEM-MVM [13] and the hybrid FEM-MMVF are the same.

Table 1. CPU time for the different studied methods [13].

	CPU time
FEM-MMVF (2500 modes)	10 mn 44 s
HFSS (77950 tetrahedrons)	4 h 43 mn

3.2. Two Complex Discontinuities $M = 2$: One-resonator Filter

Figure 4 shows a one-resonator filled with isotropic medium ($\varepsilon_r = 1.3$, $\mu_r = 1.3$) constructed by two identical complex irises distanced by a distance d. Fig. 5 shows the geometries and the meshing of one iris. To choose the number of modes used, we found in practice that the optimal way is firstly to arrange modes by ascendant cut-off frequencies. Then, we set a frequency F. Finally, we took all modes having cut-off frequencies smaller than F in all waveguides. After a convergence study we put $F = 600\,\text{GHz}$ (see Fig. 6).

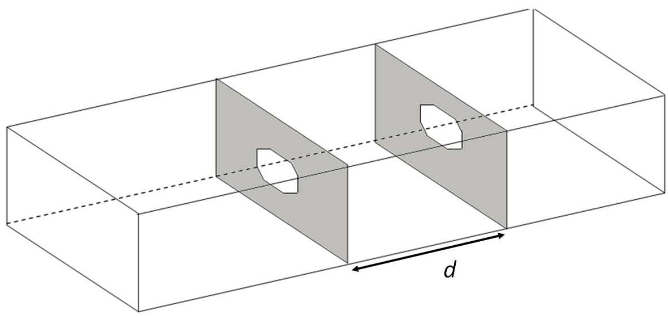

Figure 4. One-resonator filter. Waveguide WR62.

Figures 7 and 8 show the reflection coefficient of the filter for $d = 17\,\text{mm}$ and $d = 8.5\,\text{mm}$, respectively. Results obtained using the hybrid

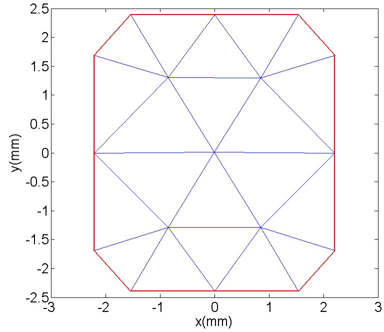

Figure 5. Geometries and meshing of the iris.

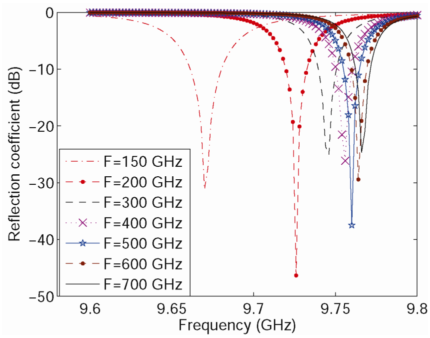

Figure 6. Convergence study of the proposed method against the number of modes ($d = 17\,\mathrm{mm}$).

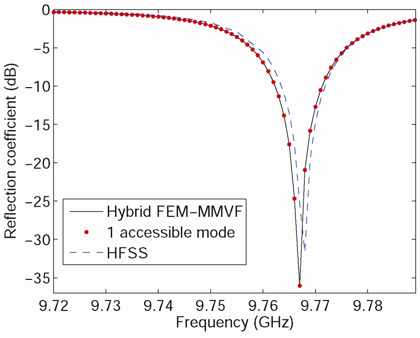

Figure 7. Reflection coefficient for various numerical methods $d = 17\,\mathrm{mm}$.

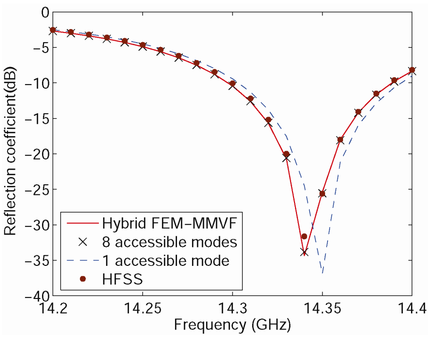

Figure 8. Reflection coefficient for various numerical methods $d = 8.5\,\mathrm{mm}$.

FEM-MMVF are compared to those achieved by HFSS and connecting the S matrices by varying the number of accessible modes. Table 2 gives an idea in time and resources of the different studied methods. In HFSS's simulations, we observe that finer mesfing surpasses the memory storage of our computer. Tables 3 and 4 give the resonant frequencies of the circuit using the different studied methods for $d = 17\,\mathrm{mm}$ and $d = 8.5\,\mathrm{mm}$, respectively. We observe that the hybrid FEM-MMVF and HFSS give the same accuracy. Nevertheless, even using all symmetries in the HFSS design, our method is considerably more rapid. When the resonator length d is sufficiently small (i.e., $d = 8.5\,\mathrm{mm}$), using the connection S matrices method, a convergence study according to the number of accessible modes must be made (see

Table 2. CPU time for the different studied methods $d = 17$ mm.

	CPU time
FEM-MMVF	14 mn 30 s
HFSS (184335 tetrahedrons and using all symmetries)	4 h 21 mn

Table 3. Resonant frequencies for various methods $d = 17$ mm.

	Resonant frequencies
FEM-MMVF	9.767 GHz
1 accessible mode	9.767 GHz
HFSS	9.768 GHz

Table 4. Resonant frequencies for various methods $d = 8.5$ mm.

	Resonant frequencies
FEM-MMVF	14.33 GHz
1 accessible mode	14.35 GHz
8 accessible mod	14.33 GHz
HFSS	14.33 GHz

Fig. 8). This convergence study is no longer necessary using our hybrid FEM-MMVF. But when the resonator length d is sufficiently large (i.e., $d = 17$ mm) one accessible mode can achieve good accuracy (see Fig. 7).

CPU time against resonator length d.

- HFSS: By decreasing the resonator length d, the number of tetrahedron elements will increase which increases the CPU time. This feature is observed in practice.
- Connecting the S matrices: if the resonator length d is sufficiently large, one accessible mode can achieve good accuracy. So that, the sizes of scattering matrices are 2×2. In this case, the FEM-MVM is more rapid than the FEM-MMVF. By decreasing the resonator length d, the number of accessible modes will increase. Thus, the dimensions of the S matrices of discontinuities will augment which increases the CPU time. In addition, a very time consuming convergence study according to the number of accessible modes must be made. We mention that in practical cases as in waveguide filters, distances between discontinuities are small. In these cases, the FEM-MMVF is more rapid than FEM-MVM.
- Hybrid FEM-MMVF: By decreasing the resonator length d, the

CPU time is steady because the total S matrix of the circuit depends only on the total number of modes in the circuits. This feature presents a great advantage against the two first numerical methods.

3.3. Three Complex Discontinuity $M = 3$: Dual Mode Filter

Dual-mode filters with square cross section find numerous applications in waveguide technology. Generally, coupling and tuning elements are introduced to rotate the original degenerated modes [16]. In our hybrid method, the shape of these elements can be either simple (i.e., rectangle) or complex.

We consider a dual-mode filter as shown in Fig. 9. The input is a rectangular waveguide (WR75) which couples to the cavity through a centered horizontal aperture of size $10\,\text{mm} \times 6\,\text{mm}$. The output of the filter is identical to the input but rotated by $\pi/2$. The dimensions of the dual-mode cavity are $14.8\,\text{mm} \times 14.8\,\text{mm} \times 25\,\text{mm}$. Four 2D square metal slabs of dimensions $(3\,\text{mm} \times 3\,\text{mm})$ and $(1\,\text{mm} \times 1\,\text{mm})$

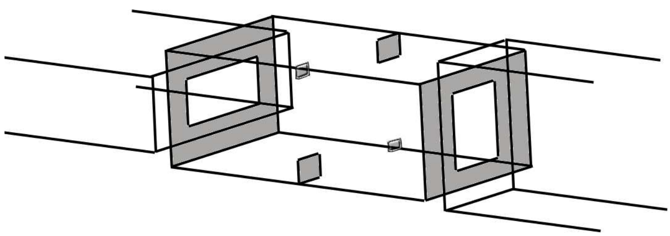

Figure 9. Dual-mode filter.

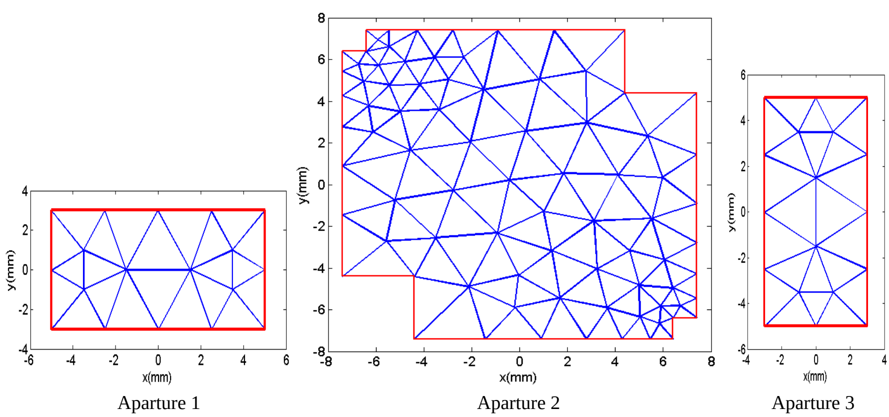

Figure 10. Geometries and meshing the three apertures.

are inserted at corners of square cavity. The position and the shape of the four 2D square metal slabs are inspired from reference [16]. Their sizes are chosen to improve the filter response. We point out that our hybrid method is versatile. It doesn't depend on the shape of discontinuities. The meshing of the three apertures is given in Fig. 10. After a convergence study (see Fig. 11), we considered all modes in the circuit of cut-off frequencies less than $F = 250\,\text{GHz}$.

Figure 12 displays the reflection coefficient versus frequency using HFSS and the proposed hybrid FEM-MMVF. We considered two isotropic media ($\varepsilon_r = 1.2$, $\mu_r = 1.2$) and ($\varepsilon_r = 1.1$, $\mu_r = 1.1$). Table 5 shows the resonant frequencies and Q-3 dB of the response using the studied methods. We obtained good agreement with the full-wave FEM based CAD tool results. Nevertheless, our hybrid method is significantly more rapid.

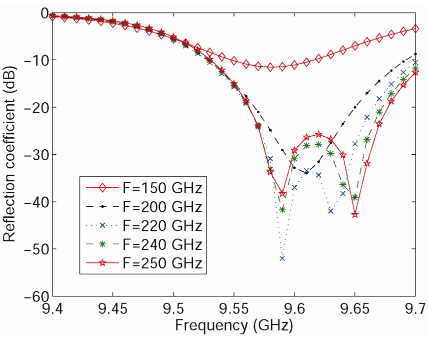

Figure 11. Convergence study of the proposed method against the number of modes ($\varepsilon_r = 1.2$, $\mu_r = 1.2$).

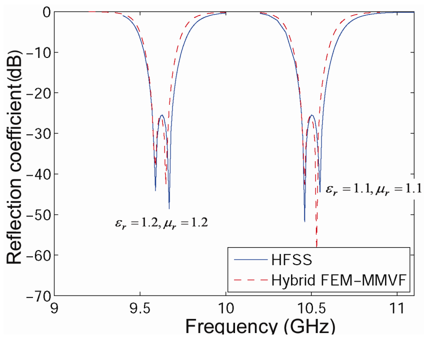

Figure 12. Reflection coefficient versus frequency of the dual mode filter.

Table 5. Resonant frequencies and Q-3 dB of the studied methods.

	Resonant frequencies		Q-3 dB
FEM-MMVF ($\varepsilon_r = 1.2$, $\mu_r = 1.2$)	9.59 GHz	9.65 GHz	31.98
HFSS ($\varepsilon_r = 1.2$, $\mu_r = 1.2$)	9.59 GHz	9.67 GHz	26.62
FEM-MMVF ($\varepsilon_r = 1.1$, $\mu_r = 1.1$)	10.46 GHz	10.53 GHz	31.91
HFSS ($\varepsilon_r = 1.1$, $\mu_r = 1.1$)	10.46 GHz	10.56 GHz	26.28

4. CONCLUSION

We propose a fast and accurate hybrid FEM-MMVF tool to the complete CAD of cascaded 2D complex discontinuities in isotropic rectangular waveguides.

The benefits of our proposed method compared to previous studied ones are observable. Firstly, the proposed hybrid method gives an overall reduction in CPU time more than 95% against HFSS in all studied structures. Secondly, compared to connecting the S matrices using the hybrid FEM-MVM, our hybrid FEM-MMVF method avoids the convergence study according to the number of accessible modes which is very time consuming.

The introduced hybrid FEM-MMVM has been accurately applied to the analysis of several application examples of highly practical interest such as cross shaped iris and dual-mode filter thus improving the computing time against FEM based CAD tools. This advantage becomes obvious especially when the circuit contains fine details.

Our hybrid method can be applied to the fast and accurate analysis of more structures containing complex discontinuities in rectangular waveguides.

REFERENCES

1. Wexler, A., "Solution of waveguide discontinuities by modal analysis," *IEEE Trans. on Microwave Theory and Tech.*, Vol. 15, No. 9, 508–517, Sep. 1967.
2. Shih, Y. C., T. Itoh, and L. Q. Bui, "Computer-aided design of millimeter-wave E-plane filters," *IEEE Trans. on Microwave Theory and Tech.*, Vol. 31, No. 9, 135–142, Feb. 1983.
3. Tao, J. W. and H. Baudrand, "Multimodal variational analysis of uniaxial waveguide discontinuities," *IEEE Trans. on Microwave Theory and Tech.*, Vol. 39, No. 3, 506–516, Mar. 1991.
4. Lilonga, D., J. W. Tao, and T. H. Vuong, "Uniaxial discontinuities analysis by a new multimodal variational method: Application to filter design," *International Journal of RF and Microwave Computer-Aided Engineering*, Vol. 17, No. 1, 77–83, Dec. 2006.
5. Jin, J., *The Finite Element Method in Electromagnetics*, 2nd edition, John Wiley & Sons, New York, 2001.
6. Bayer, R. and F. Arndt, "Efficient modal analysis of waveguide filters including the orthogonal mode coupling elements by a MM/FE method," *IEEE Microwave Guided Wave Lett.*, Vol. 5, No. 1, 9–11, Jan. 1995.

7. Arndt, F., et al., "Automated design of waveguide components using hybrid mode-matching/numerical EM building-blocks in optimization-oriented CAD frameworks — State-of-the-art and recent advances," *IEEE Trans. on Microwave Theory and Tech.*, Vol. 45, No. 5, 747–760, May 1997.
8. Arndt, F., et al., "Fast CAD and optimization of waveguide components and aperture antennas by hybrid MM/FE/MoM/FD methods-state-of-the-art and recent advances," *IEEE Trans. on Microwave Theory and Tech.*, Vol. 52, No. 1, 292–305, Jan. 2004.
9. Arena, D., M. Ludovico, G. Manara, and A. Monorchio, "Analysis of waveguide discontinuities using edge elements in a hybrid mode matching/finite elements approach," *IEEE Microwave and Wireless Components Lett.*, Vol. 11, No. 9, 379–381, Sep. 2001.
10. Sheng, X. Q., K. W. Leung, and E. K. N. Yung, "Analysis of waveguide-fed dielectric resonator antenna using a hybrid finite element method/moment method," *IEEE Microwaves, Antennas and Propagation*, Vol. 151, No. 1, 91–95, Feb. 2004.
11. Bertini, S., A. Monorchio, and M. Bandinelli, "Efficient design of horn antennas by hybridizing mode matching/FEM with MoM," *International Conference on Electromagnetics in Advanced Applications*, 868–871, Sep. 17–21, 2007.
12. Sun, J. and C. Zhang, "Transmission characteristics analysis for mine tunnel with metallic wind bridge using hybrid MM/FEM approach," *Asia-Pacific Microwave Conference*, Vol. 4, Dec. 4–7, 2005.
13. Yahia, M., J. W. Tao, H. Benzina, and M. N. Abdelkrim, "Analysis of complex rectangular waveguide discontinuities using hybrid MVM-FEM," *Asia-Pacific Microwave Conference*, 111–114, Dec. 2009.
14. Yahia, M., J. W. Tao, H. Benzina, and M. N. Abdelkrim, "Complex 2D discontinuities analysis using hybrid finite element method and a modified multimodal variational formulation-application to filter design," *European Microwave Conference*, 1301–1304, Sep. 26–Oct. 1, 2010.
15. Marcuvitz, N., *Waveguide Handbook*, McGraw-Hill, New York, 1951.
16. Amari, S., "Application of representation theory to dual-mode microwave bandpass filter," *IEEE Trans. on Microwave Theory and Tech.*, Vol. 57, No. 3, 430–441, Feb. 2009.